Pressure Solution at the Molecular Scale

Edgar Alejandro Pachon-Rodriguez, Agnès Piednoir, Jean Colombani

Pressure Solution at the Molecular Scale

Edgar Alejandro Pachon-Rodriguez, Agnès Piednoir, and Jean Colombani*

Laboratoire de Physique de la Matière Condensée et Nanostructures; Université de Lyon; Université Claude Bernard Lyon 1; CNRS, UMR 5586; Domaine scientifique de la Doua, F-69622 Villeurbanne cedex, France

(Received 26 May 2011; published 30 September 2011)

The topological evolution of the cleavage surface of a gypsum single crystal during its dissolution in a flowing undersaturated aqueous solution has been observed with an atomic force microscope. The matter transfer from solid to liquid proceeds through the migration of atomic steps. The step velocity has been measured and appears to depend on the force applied by the tip on the surface. Whereas the high force velocity enhancement is likely to stem from corrosive wear, the speed behavior at low force (< 10 nN) differs drastically and can be interpreted as a consequence of the pressure solution of the crystal induced by the tip force. The step velocity evolution with the force obeys the known kinetic law of pressure solution. Hence these experiments enable us to evidence a first atomic mechanism at the origin of pressure solution.

DOI: 10.1103/PhysRevLett.107.146102 PACS numbers: 68.08.−p, 62.20.Hg, 68.37.Ps, 91.60.Gf

If water is present between two solids pressed together, the stress at the contact induces local dissolution, diffusion of the dissolved species out of the interface and precipitation on less stressed surfaces. The driving force is the stress-induced chemical potential gradient in the solid. This dissolution-diffusion-precipitation sequence, known as ''pressure solution,'' may cause creep of the contact, or lead to the sticking of the solids. The first phenomenon is known to play a leading role in Earth's upper crust, during tectonic deformation or during the consolidation of active fault gouges following earthquakes [1], and to be responsible for the wet creep of minerals [2]. The second phenomenon contributes largely to the diagenesis of sedimentary rocks (transition from loose sediments to cohesive solids) [1]. Despite its importance, the understanding of pressure solution is far from complete. For instance, the nature of the solid contact during pressure solution has become clearer, with slowly growing solid-solid interfaces containing nanometric water films, separated by micrometric channels [3–6]. But large morphologic changes of the free surfaces of stressed crystals in saturated solution have been pointed out, which suggests a strong interplay between dissolution in the confined fluid film and at the free surfaces [7].

Besides, much progress has been made during the last decade in our understanding of the molecular mechanisms taking place at the solid-liquid interface during normal dissolution. The existence of a surface-normal retreat [8], the role of etch pits as step train source [9], the influence of the surface history [10], etc., have been evidenced. These advances have been made possible by the use of techniques resolving nanometric objects, like atomic force microscopy (AFM) or vertical scanning interferometry (VSI). The molecular kinetics during pressure solution has not been investigated with such tools yet, although the knowledge of its basic mechanisms is necessary to achieve a comprehensive understanding of the phenomenon.

In this Letter, using an AFM tip successively to apply a stress to a dissolving mineral surface and to probe its dynamics, we measure the kinetics of a molecular mechanism of pressure solution, namely, the motion of atomic steps. Thereby we demonstrate that it obeys the expected thermodynamic law of pressure solution, hence making a link between the molecular process and the resultant macroscopic phenomenon.

To be able to isolate the role of pressure on dissolution from other influences, we need a mineral with (i) dissolution rates measurable in laboratory times, (ii) a chemical reaction as simple as possible, to focus on the topological aspect of dissolution, and (iii) dissolution proceeding through a well-defined mechanism. Gypsum ($CaSO_4$, $2H_2O$) fulfills these three criterions, because it dissolves in accessible times [11], its reaction depends little on pH and P_{CO_2} [12], and the matter detachment is partly achieved by the migration of well-known atomic steps [13]. Gypsum was one of the first materials imaged with AFM [14]. Its lattice is monoclinic with layers of SO_4^{2-} tetrahedra bound to Ca^{2+} cations, alternating with water layers. This structure displays a perfect (010) cleavage plane in the middle of the water layers. All the investigated surfaces come from freshly cleaved samples of a transparent natural gypsum single crystal. The calcium sulfate aqueous solutions where the samples dissolve were obtained in dissolving calcium sulfate powder in ultrapure water until saturation, and diluting the solution to the desired concentration. The saturation index Ω is computed as $(c/c_{sat})^2$, c being the concentration of Ca^{2+} and SO_4^{2-} and c_{sat} the solubility of gypsum in water.

In the atomic force microscope, a sharp Si_3N_4 tip is attached near the free end of a cantilever. When brought in close proximity with a surface, forces arise between the tip and the sample, detected by the deflection of the cantilever. We have used the microscope in contact mode, where a feedback loop continuously changes the vertical

position of the tip to keep the surface-tip repulsion force constant, which provides a relief recording of the surface [cf. Fig. 1(a)]. The measurements have been carried out in a fluid cell, where an aqueous solution undersaturated in gypsum is injected continuously by a pump. The flow enables us to keep the resultant concentration field above the surface constant during the experiment. The flow rate of 0.3 mL/ min has been chosen as the highest one provoking no disturbance of the AFM signal.

For the atomic step speed measurement, the scan angle is first changed in order to bring the investigated step parallel to the y axis. The scan of this axis is disabled, and the tip then moves back and forth along one segment of the x axis, with a 1 Hz frequency. The resultant image is a time-position representation of the step [cf. Fig. 1(b)]. The step velocity is subsequently computed from the angle between the trace left by the step motion and the y axis [13]. This spatiotemporal representation provides much better accuracy than the mere comparison of the step position between two subsequent topographic images. It has been noticed that the step speed tends to decay when the step density increases. The dissolution kinetics stems from a combination of the kinetics of the ion detachment from the surface, of the diffusion of the solute from the surface to the bulk, and of the local convective motions induced by the tip motion in the solution [15]. The presence of numerous moving steps in a region may induce a local increase of the concentration, before the evacuation of the solute by diffusion and convection, so give rise to a fall of the driving force of the reaction and to a slowing down of the step motion. Accordingly, all step velocities have been measured in regions with a low step density, preferentially for isolated steps.

Whereas no evolution is observable in air, the surface cleans up and curved steps defining irregular regions disappear during the minutes following the introduction of the sample in the fluid cell. This first stage leads to a geometrical topography constituted of shallow etch pits [cf. Fig. 1(a)]. All of them are parallelograms, with an obtuse angle of about 118°, corresponding to the angle between the a and c axes of the monoclinic lattice of gypsum [14]. The crystallographic directions forming the boundary of the etch pits have been rigorously identified as being always [100] and [001] [13]. These etch pits broaden by translation of their enclosing steps. This enlargement leads invariably to an elongated shape of the pits, due to the anisotropy of the steps velocity. The [100] steps move faster than the [001] ones, leading to [001] edges much longer than [100] ones. The majority of the steps displays a height of about 0.75 nm, corresponding to one half of the b axis parameter (0.76 nm) and to the height of one molecular motif. Higher steps are also often observed, with a height being a multiple of 0.76 nm, but we concentrate here exclusively on the speed of steps of height $b/2$, to focus on one single topologic mechanism. For the same reason, we have limited our investigation to the [001] steps, their velocity being lower than the [100] ones, thus facilitating the observation of their pressure-induced enhancement. Deep etch pits are never observed. This surprising feature is a consequence of the existence of irregular high-speed step trains sweeping the surface and eroding the existing pits. Fan & Teng have suggested that these [u0w] steps correspond to highly unstable crystallographic directions, close to [101] [13].

Figure 2 displays the velocity of steps [001] and [100] for various saturation indices from our experiments and reported in the literature. The anisotropy of the reaction appears clearly, the speed of the two directions exhibiting a discrepancy of about 1 order of magnitude. Both show a decaying trend when the saturation is approached, with a rather large dispersion of the values. This dispersion may derive from the variation of the force applied by the tip

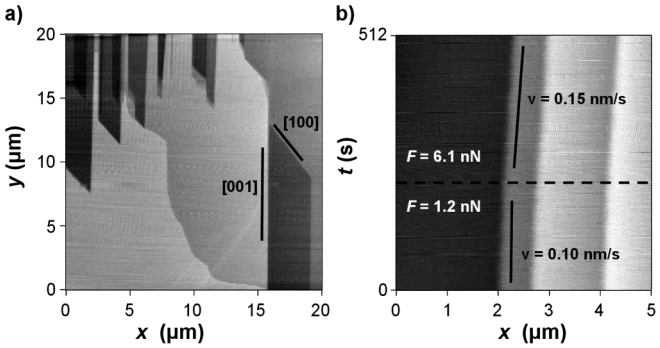

FIG. 1. (a) AFM image of the (010) face of a gypsum single crystal experiencing dissolution in a flowing calcium sulfate aqueous solution with $\Omega = 42\%$ (relief height: 5 nm). (b) Space-time representation of the migration of a [001] step for $\Omega = 88\%$ (relief height: 2 nm). The consequence of a change of the force applied by the tip is also shown.

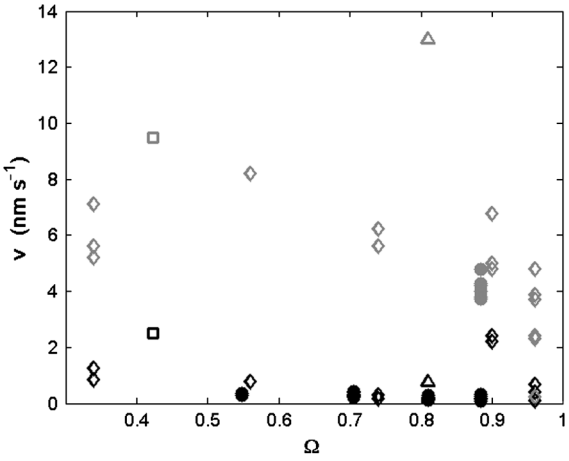

FIG. 2. Evolution with the saturation index of the step velocity in the [001] (black dots) and [100] (grey dots) directions. The results of Bosbach & Rammensee [20] (triangles), Hall & Cullen [21] (squares) and Fan & Teng [13] (diamonds) have been added to ours (circles).

during the measurement, for which no information is given in the mentioned works. To estimate this effect, the set-point value of the repulsive force between the tip and the surface has been changed in the middle of the spatio-temporal acquisition of a step motion. As can be seen in Fig. 1(b), this action induces an immediate change of the (t, x) slope, corresponding to a sudden change of the step velocity. Accordingly we have carried out systematic velocity measurements in the [001] direction for varying forces applied by the AFM tip on the surface and various saturation indices. Figure 3 shows that for each saturation state, the force increase always results in a velocity rise, with a decaying slope.

Wear studies have already reported mechanically enhanced dissolution in calcite [16,17]. In experiments similar to ours where the AFM tip moves back and forth along a segment crossing an atomic step at the cleavage surface of a calcite single crystal, a growing wear track is observed. The wear is attributed to the promotion, by the tip-induced strain, of kink sites creation at the point where the tip crosses the step, and its growth rate is exponential [17]. To establish if we face the same wear phenomenon, velocity measurements at higher forces have been carried out. Two new features are encountered. First, whereas the [001] steps were always observed to remain straight during migration, for applied forces above about 10 nN, the tip route-atomic step intersection becomes a parallelogram corner, and the step migrates parallel to the [001] line on one side of the tip and parallel to the [100] line on the other (cf. Fig. 4). Second, in this force range, the evolution of the velocity of the step with the applied force exhibits a behavior distinctly at variance with the one at low force, with a slightly growing slope, as shown in Fig. 4.

Therefore a threshold exists between two dissolution enhancement regimes. The high force behavior can be ascribed to an atomic wear phenomenon, in which the absence of wear track, present in the case of calcite, could derive from a more unstable nature of the kink sites in the gypsum steps. Below this stage, another process takes place with much smaller step velocities. We attribute this low force regime to the pressure solution of the mineral under the influence of the tip. During the passage of the tip at the level of the investigated step, the stress state of the solid is modified. To get an estimate of this state, a Hertzian contact has been considered between the tip and the surface. In this framework, the compressive stress is maximum under the tip, where it writes $P_0 = (1/\pi)\{6FE^2/[(1-\nu^2)^2 r^2]\}^{1/3}$, with F the applied force, E and ν Young's modulus and Poisson's ratio of gypsum, and r the radius of curvature of the tip. Taking $E = 45$ GPa, $\nu = 0.33$, $r = 40$ nm and $F = 10$ nN, we find $P_0 = 1.5$ GPa. This value is large enough to be likely to hinder the solvation of the ions, thus impeding the step to move forward. But the applied force also creates a strain field around the tip. The resultant chemical potential of the crystal surrounding the tip can be written $\mu_S = \mu_0 + \delta U_e + \delta U_p + \delta U_s$, where μ_0 stands for the chemical potential of the unstressed solid, δU_e and δU_p for the elastic and plastic strain energy of the solid, and δU_s for the surface energy [18]. It can be noted that no contribution of the work of the pressure forces is present in this expression, the liquid pressure above the surface outside the contact remaining always the atmospheric pressure and the normal stress in the solid outside the Hertzian contact being zero. Except for the step migration, no irreversible strain is observed in the course of the AFM tip, and the investigated surfaces always remain plane, so the plastic

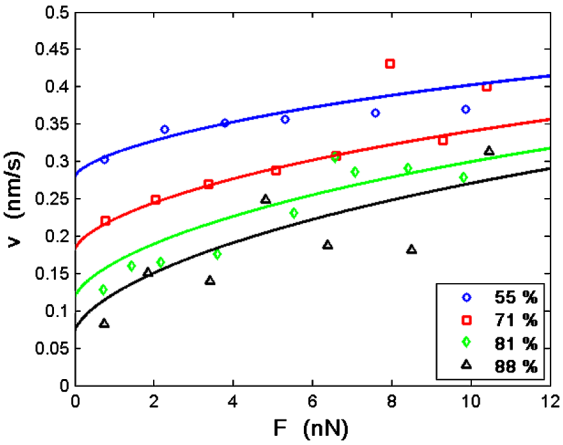

FIG. 3 (color online). Step velocity in the [001] direction as a function of the force applied by the AFM tip on the surface for various saturation indices. Each dot stands for an average of a few values. The curves are a fit of the experimental values by a law based on the inclusion of strain energy in the transition state theory.

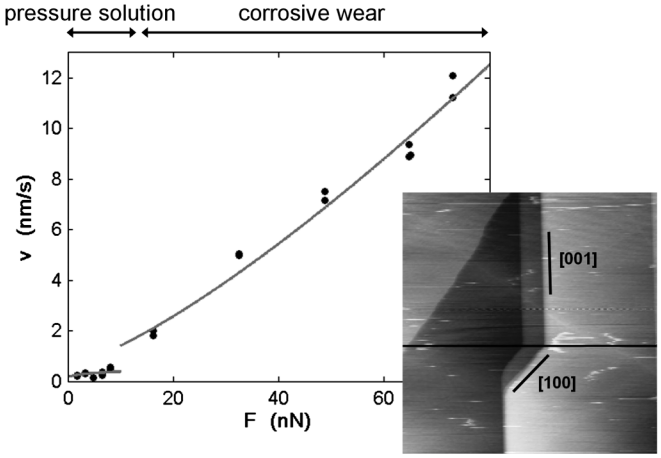

FIG. 4. Step velocity in the [001] direction for large forces applied by the AFM tip on the surface and for $\Omega = 71\%$. Curves are guides for the eyes. Insert: AFM topographic image at the end of the 32 nN velocity measurement (15×15 μm^2, relief height: 5 nm). The black segment indicates the tip route during the velocity measurement.

and surface energy terms can be neglected. The maximum tensile stress, at the contact periphery, is $\sigma = (1 - 2\nu)P_0/3$, and results in a stored molar elastic energy $\delta U_e = \sigma^2 \bar{V}/(2E)$, with $\bar{V}$ the molar volume of gypsum. Knowing $\bar{V} = 7.5 \times 10^{-5}$ m^3/mol, we find $\sigma = 160$ MPa and $\delta U_e = 2.3 \times 10^{-2}$ kJ/mol. To catch the influence of this mechanical energy on the liquid-solid equilibrium, one can evaluate the solubility in bulk water of gypsum in this stress state by $c^{\sigma}_{\mathrm{sat}} = c_{\mathrm{sat}} \exp(\delta U_e/(RT))$. An increase of about 1% is found, as is usual in pressure solution studies [18].

Focussing exclusively on step retreat, the transition state theory (TST) of dissolution should apply. According to the TST, the advancement rate of the reaction should take the form $d\xi/dt \sim [1 - \exp(\mathcal{N}\Delta G/(RT))]$ where ΔG is the Gibbs free energy of the overall reaction, R the gas constant, T the temperature and $\mathcal{N}$ the number of elementary reactions [19]. For gypsum dissolution, $\mathcal{N}$ has often been measured equal to one [13]. If the system is exclusively driven out of equilibrium by the undersaturation of the aqueous solution, we have $\Delta G = RT \ln\Omega$. As step migration is at the origin of the matter removal, the step speed v should follow to some extent the TST law and one should simply have $v \sim (1 - \Omega)$. As can be seen in Fig. 2, v and Ω are not simply related by a linear law. So we have included an elastic perturbation in the TST law to get a correct modelization of our experiments. The derivation of the exact TST expression is a nontrivial task, requiring the solution of the nonhomogeneous thermodynamical and mechanical local equilibrium. At first order, we can introduce a mechanical contribution in the Gibbs free energy: $\Delta G = RT \ln\Omega - \Delta U_e$. The elastic strain term ΔU_e derives from the molar elastic energy δU_e stored during the tip crossing, so $\Delta U_e \sim \sigma^2 \bar{V}/(2E)$. Thereby the step velocity can be written as $v = v_{\mathrm{lim}}\{1 - \Omega \exp[-\alpha\sigma^2 \bar{V}/(2ERT)]\}$, with α a geometric factor depending on the shape of the elastic strain field around the contact and v_{lim} an asymptotic velocity. A fit of all the experimental values with this law is shown in Fig. 3, with α and v_{lim}, common to all saturation indices, as only fitting parameters. The experimental and theoretical values are found to agree. Thus considering that the tip influence on the solid lies in an elastic strain contribution to its chemical potential gives the correct scaling of the dissolution enhancement, thereby validating the hypothesis of local pressure solution.

As a summary we have observed with atomic force microscopy that the velocity of the atomic steps on the surface of a dissolving gypsum single crystal depends on the force applied by the tip. For forces greater than 10 nN, the velocity evolution with force is comparable to the tribological enhancement of dissolution observed in calcite. For smaller forces, the step speed evolution with force exhibits a completely different behavior and can be interpreted as the consequence of the pressure solution of the crystal under the influence of the tip. Besides the fact that this observation opens the way to a more quantitative use of AFM for the study of liquid-solid interfaces, it constitutes a first link between the macroscopic description of pressure solution and the atomistic processes underlying its kinetic laws. The relation obtained here should be applicable to all pressure solution phenomena by step retreat, so it should help, in particular, in evaluating more quantitatively the free-face contribution in pressure solution studies [6], or to find additives against the wet creep of polycrystalline ceramics [2].

We thank Elisabeth Charlaix, Lydéric Bocquet, François Renard, and Dag Dysthe for fruitful discussions. This work was supported by Lafarge Centre de Recherche, Région Rhône-Alpes and CNES (French space agency).

*Jean.Colombani@univ-lyon1.fr

[1] D. K. Dysthe, Y. Podladchikov, F. Renard, J. Feder, and B. Jamtveit, Phys. Rev. Lett. **89**, 246102 (2002).
[2] E. Pachon-Rodriguez, E. Guillon, G. Houvenaghel, and J. Colombani (to be published).
[3] S. denBrok, Geology **26**, 915 (1998).
[4] D. K. Dysthe, F. Renard, J. Feder, B. Jamtveit, P. Meakin, and T. Jossang, Phys. Rev. E **68**, 011603 (2003).
[5] N. Alcantar, J. Israelachvili, and J. Boles, Geochim. Cosmochim. Acta **67**, 1289 (2003).
[6] D. Koehn, A. Malthe-Sorenssen, and C. Passchier, Chem. Geol. **230**, 207 (2006).
[7] J. Bisschop and D. K. Dysthe, Phys. Rev. Lett. **96**, 146103 (2006).
[8] A. Luttge, E. Bolton, and A. Lasaga, Am. J. Sci. **299**, 652 (1999).
[9] A. Lasaga and A. Luttge, Science **291**, 2400 (2001).
[10] A. Luttge, J. Electron Spectrosc. Relat. Phenom. **150**, 248 (2006).
[11] J. Colombani and J. Bert, Geochim. Cosmochim. Acta **71**, 1913 (2007).
[12] A. Jeschke, K. Vosbeck, and W. Dreybrodt, Geochim. Cosmochim. Acta **65**, 27 (2001).
[13] C. Fan and H. Teng, Chem. Geol. **245**, 242 (2007).
[14] H. Shindo, M. Kaise, H. Kondoh, C. Nishihara, H. Hayakawa, S. Ono, and H. Nozoye, J. Chem. Soc. Chem. Commun. **16**, 1097 (1991).
[15] J. Colombani, Geochim. Cosmochim. Acta **72**, 5634 (2008).
[16] N. Park, M. Kim, S. Langford, and J. Dickinson, Langmuir **12**, 4599 (1996).
[17] N. Park, M. Kim, S. Langford, and J. Dickinson, J. Appl. Phys. **80**, 2680 (1996).
[18] F. Renard, A. Park, P. Ortoleva, and J. Gratier, Tectonophysics **312**, 97 (1999).
[19] J. Schott, O. S. Pokrovsky, and E. H. Oelkers, Rev. Mineral. Geochem. **70**, 207 (2009)
[20] D. Bosbach and W. Rammensee, Geochim. Cosmochim. Acta **58**, 843 (1994).
[21] C. Hall and D. Cullen, AIChE J. **42**, 232 (1996).